I&EC research
Industrial & Engineering Chemistry Research

Article

Cite This: Ind. Eng. Chem. Res. 2019, 58, 5445−5454

pubs.acs.org/IECR

Kinetic Study of Belite Formation in Cement Raw Meals Used in the Calcium Looping CO_2 Capture Process

Mónica Alonso, José Ramón Fernández,* and Juan Carlos Abanades

Spanish Research Council, INCAR-CSIC, Francisco Pintado Fe, n. 26, 33011 Oviedo, Spain

ABSTRACT: Calcium looping technology could be one of the most efficient ways to drastically reduce the carbon footprint of cement manufacture since $CaCO_3$ is a major component of the raw meal used to produce clinker. However, calcined raw meal can be a poor CO_2 sorbent due to the fact that the formation of Ca_2SiO_4 (belite) causes a reduction in the amount of free CaO. Effective reaction rates for the formation of belite from both $CaCO_3$ and CaO (i.e., after calcination) were obtained in this work for different raw meals with similar compositions but very different levels of Ca−Si aggregation. Tests carried out in thermogravimetric analyzers revealed that belite can be formed quickly, even with calcination periods of about 1 min. The 3D-diffusion model proposed by Jander and Hoffmann [Jander, W.; Hoffmann, E. Reaktionen im festen Zustande bei höheren Temperaturen. XI. Mitteilung. Die Reaktion zwischen Calciumoxyd und Siliciumdioxyd. *Z. Anorg. Allg. Chem.* **1934**, *218*, 211−223] represents reasonably well the conversion of the solids to belite in marl-type raw meals at temperatures between 800 and 900 °C. The activation energy calculated in this temperature range (i.e., 325 kJ/mol) is consistent with the data reported in the literature on belite formation in CaO/SiO_2 materials at higher temperatures. The differences in the reaction rates between the materials are due to the pre-exponential factors, related to the level of aggregation of Ca and Si in the materials. The information on this topic will help to predict the decrease in the CO_2 sorption capacity of the calcined raw meals used in calcium looping systems integrated in cement plants.

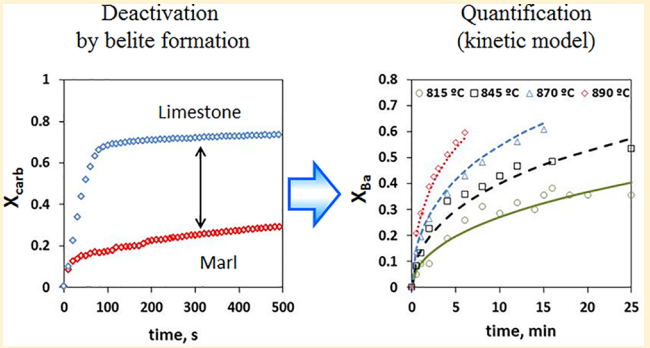

INTRODUCTION

The cement sector is the second-largest industrial emitter of CO_2 (with a share of around 27% in this segment) and is responsible for about 8% of global man-made CO_2 emissions (i.e., 2.2 Gt CO_2 per year), the largest share of which (1.5 Gt CO_2) is caused by the decomposition of carbonates.[1] To meet the objectives agreed at COP22, this sector must find a way to match the increasing demand for cement with a dramatic reduction in CO_2 emissions. Although a range of technical improvements along the production line[2] can help to reduce emissions, there is clearly a need to adopt CO_2 capture and storage technologies to address excessive emissions of CO_2 from the manufacture of clinker.

Until now, most of the effort directed at CO_2 capture in cement plants has been focused on oxy-fuel combustion and postcombustion (mainly by amine scrubbing) technologies.[2,3] However, the synergy that exists between the calcium looping (CaL) and cement production makes this emerging technology one of the most promising alternatives for capturing CO_2 in cement plants.[2,4−7] In calcium looping, the CO_2 present in combustion environments is separated by its reaction with CaO-based sorbents over successive carbonation/calcination cycles at high temperatures. Over the past 2 decades, calcium looping has undergone extensive progress in relation to the development of sorbents, process modeling, and experimental testing, especially focused on the decarbonization of the power generation sector,[8−11] resulting in successful pilot plant demonstrations up to 1−2 MW scale.[12−16] By operating at very high temperatures and using the CaO-based material purged from the calciner as feedstock for clinker production, it should be possible to achieve a strong synergy between the CaL technology and cement production.[17−19] Different CaL process configurations at diverse levels of integration in cement plants have been evaluated.[7,20−30] However, very few studies contain experimental information on CaL reactors operated under the typical conditions of cement plants (i.e., small particle sizes, low gas/solid contact times, high CO_2 concentrations in the flue gas, and high CO_2 sorption capacities compared to CaL systems integrated in power plants).[31−33]

It has been widely reported that calcium-based sorbents gradually lose their CO_2 capture capacity as they are subjected to successive carbonation/calcination cycles due to solids sintering.[8,10,34,35] The decrease in solids activity is compensated for by a makeup flow of fresh sorbent, which is an important design parameter of the system. At the highest level of integration between the CaL system and the cement plant,

Received: February 11, 2019
Revised: March 21, 2019
Accepted: March 22, 2019
Published: March 22, 2019

DOI: 10.1021/acs.iecr.9b00813
Ind. Eng. Chem. Res. 2019, 58, 5445−5454

the raw meal itself, which is typically composed of around 80 wt % of $CaCO_3$, acts as the calcium-based sorbent.[36] However, there is very little experimental evidence to confirm the effectiveness of cement raw meal as a CO_2 capture sorbent.[37−39] It is well-known that belite (Ca_2SiO_4) can be produced under typical cement precalciner conditions either via the direct reaction of $CaCO_3$ with SiO_2 (eq 1) or via the reaction of CaO with SiO_2 (eq 2).[40]

$$2CaCO_3 + SiO_2 \rightarrow Ca_2SiO_4 + 2CO_2 \quad (1)$$

$$2CaO + SiO_2 \rightarrow Ca_2SiO_4 \quad (2)$$

These are solid-state reactions, intermediate between other reactions that give rise to different calcium silicate phases ($3CaO{\cdot}SiO_2$, etc.) of great relevance to cement production.[41] However, the formation of belite impedes the use of cement raw meal as CO_2 sorbent because it eliminates a substantial fraction of the free CaO resulting from the calcination of natural limestones.[37,38] Larger amounts of belite are produced at high temperatures, long calcination times, and high Ca−Si aggregation levels (e.g., natural marls).[37,38] As this reaction is probably the main cause of deactivation of cement raw meals, a kinetic model that represents this reaction is essential for an accurate design of the CaL system. It can also be used to screen out different raw meal feedstocks for their application in calcium looping if they exhibit very different formation kinetics.[38]

The formation of belite (and other calcium silicates) from cement raw meals during the production of clinker has been studied in previous works.[41,42] However, they do not provide reliable information on the kinetics of this reaction at temperatures relevant for calcium looping systems (i.e., nearly 900 °C). Hence, this paper presents a kinetic study on belite formation for two raw meals with similar compositions and particle sizes but very different Ca−Si aggregation levels. Effective reaction rates for the formation of belite from $CaCO_3$ and CaO (i.e., before and after calcination, respectively) have been obtained at temperatures between 800 and 920 °C.

EXPERIMENTAL SECTION

Materials. Two raw meals commonly used in cement plants (RM1 and RM2) were tested. RM1 is a natural marl, whereas RM2 is a mixture of a limestone (LS) and a marl (MR). The limestone (LS) and the marl (MR) were milled and sieved to obtain similar particle size distributions to the raw meals and so minimize the effect of the particle size on the reaction study. The chemical compositions of these materials were measured by X-ray fluorescence using a SRS 3000 Bruker spectrometer. As can be seen in Table 1, the composition of both raw meals is similar. RM1 and RM2 contain CaO and SiO_2 in quantities of around 42 and 14 wt %, respectively. Insofar as the individual components of RM2 are concerned, LS is an almost pure limestone, whose main impurity is $MgCO_3$, whereas MR is a marl with CaO and SiO_2 contents of 37 and 21 wt %, respectively. The results show that RM2 is a binary mixture composed predominantly of 72 wt % MR and 28 wt % LS.

Because particle size is an important parameter in solid−solid and gas−solid reactions, the particle size distributions (PSDs) of the solid samples were determined by laser diffraction using a Beckman-Coulter LS 13320 analyzer. As Figure 1a shows, the RM1 sample shows a homogeneous particle size distribution that is characteristic of a single compound. However, RM2 exhibits different volumetric fractions that can be clearly separated into specific particle size ranges, as one would expect of a mixture of individual compounds (Figure 1b). The Sauter mean diameter (dp_s) and dp_{50} are 6 and 9 μm, respectively, for the two raw meals. Moreover, very similar PSDs for the individual components of RM2 (i.e., MR and LS) were obtained once they were milled and sieved (Figure 1c and Figure 1d). Consequently, the behavior of the materials tested in this study should not be affected by particle size.

Table 1. Chemical Compositions of the Solid Samples, As Determined by XRF

	composition (wt %)			
oxide	RM1	RM2	MR	LS
Na_2O			0.24	
MgO	0.65	1.26	1.23	1.87
Al_2O_3	4.09	3.56	4.86	0.22
SiO_2	13.39	15.21	21.03	0.37
P_2O_5		0.10	0.05	
K_2O	0.89	0.57	0.97	0.05
CaO	42.72	41.50	37.09	53.26
TiO_2	0.18	0.16	0.22	
Fe_2O_3	1.94	2.13	1.65	0.06
SO_3	1.04	0.30	0.45	0.10
MnO		0.08	0.08	
SrO		0.08	0.10	0.02
ZrO_2		0.02	0.02	
LOI[a]	35.01	35.26	32.17	44.06

[a]Loss on ignition.

X-ray diffraction (XRD) analyses were also carried out to identify the Ca−Si phases formed during the calcination of the samples. Diffraction measurements were obtained using a Siemens diffractometer fitted with a Cu Kα monochromatic tube. The experimental procedure consisted of step scanning at steps of 0.02°, 2 s, in the 2θ range between 5° and 90°. Samples of about 15 mg of RM1, RM2, and MR were calcined at 900 °C in air for 10 min. The X-ray spectra of the solids before and after calcination are presented in Figure 2.

As can be seen, very similar results were obtained for fresh RM1 and RM2, whose highest peak intensities correspond to $CaCO_3$ and SiO_2. $CaAl_2(Si_2Al_2)O_{10}(OH)_2$ was also identified in both fresh raw meals. In the calcined samples, less SiO_2 was detected and the main calcium silicate formed was Ca_2SiO_4 (belite), in addition to very small amounts of Ca_3SiO_5, $CaSiO_3$, and $CaO_x(Al_2O_3)_{11}$. It is for this reason that the formation of belite under the typical conditions of calcium looping must be studied in depth as the presence of belite is the main determining factor of raw meal deactivation during carbonation/calcination.

Experimental Setup and Methods. The experiments were designed bearing in mind that under the CO_2-rich conditions of a calcium looping calciner, belite can form either from the direct reaction of $CaCO_3$ with SiO_2 (eq 1) or from the reaction of CaO with SiO_2 (eq 2). Three types of studies were carried out using the above-referenced materials: the evolution of the CO_2 carrying capacity during the calcination−carbonation cycles, the kinetics of belite formation resulting from the direct reaction of $CaCO_3$ with SiO_2 (i.e., before calcination), and the kinetics of the belite formation from bringing CaO into contact with SiO_2 (i.e., after calcination). Two thermogravimetric analyzers (TGAs) were used for these tests. A commercial TA-Q5000IR apparatus was used in the

DOI: 10.1021/acs.iecr.9b00813
Ind. Eng. Chem. Res. 2019, 58, 5445−5454

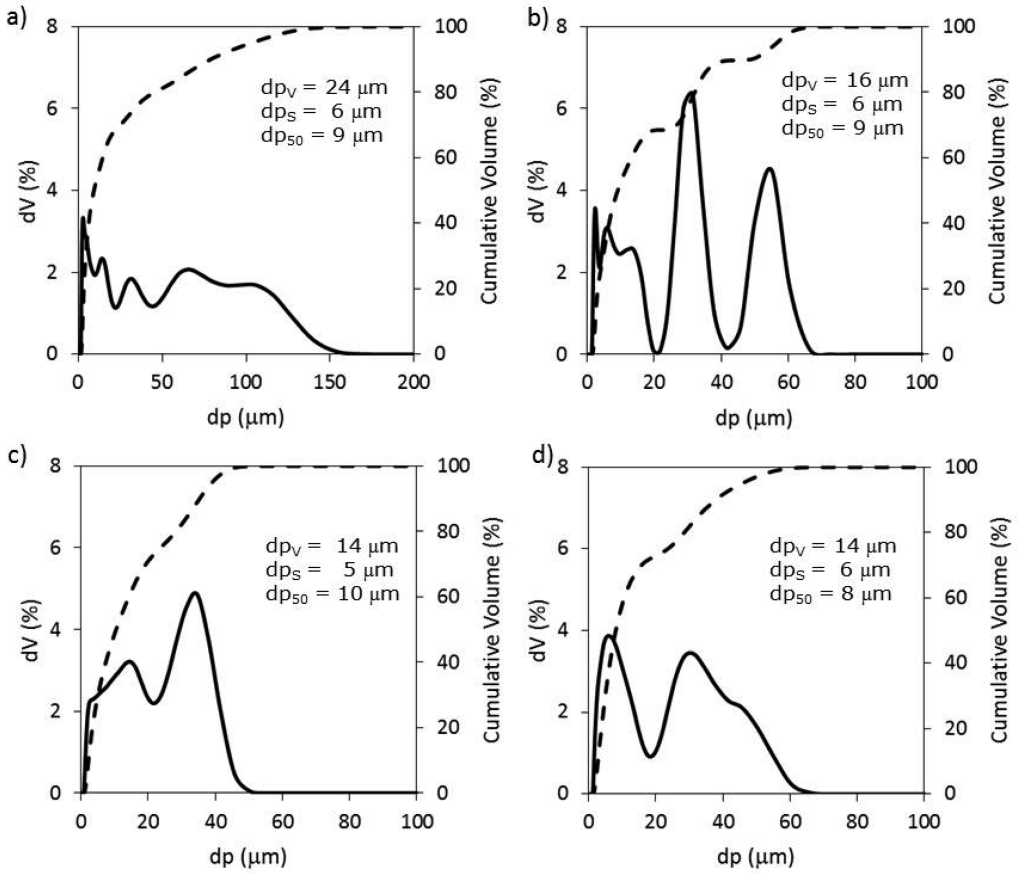

Figure 1. Particle size distributions of the solid samples as measured by laser diffraction: (a) RM1, (b) RM2, (c) MR, (d) LS.

nonisothermal tests to study the formation of belite from $CaCO_3$ (i.e., before the calcination of the raw meal). This equipment is fitted with a thermally controlled head balance, an infrared oven that can achieve programmable heating rates up to 500 °C/min, and a baseline dynamic drift of less than 10 μg (after correction by means of a blank test). Another in-house TGA (described in detail elsewhere[43]) was used to study reactions under isothermal conditions. In these tests, it is possible to deduce the type of reaction from the conversion vs time curves (whereas in nonisothermal tests this is not possible as the plots always follow sinusoidal-type curves). Moreover, the reaction rate equations provide analytical solutions for the main mechanisms known. For this reason, isothermal studies were carried out whenever possible (i.e., in the tests designed to study the formation of belite from CaO and the CO_2 carrying capacity of calcined samples). In the in-house TGA, the solids were introduced into a platinum basket, located inside a mullite tube with an external diameter of 0.025 m and heated by two electrical ovens (one of which was employed for gas preheating purposes). The reactant gases were fed in at the bottom of the tube, and mass-flow controllers regulated the flow rates. The evolution of the weight and temperature of the samples was continuously monitored during the tests.

The cyclic experiments aimed at evaluating the CO_2 carrying capacity of the solids were carried out with initial sample weights of about 10 mg. This amount of solids, which is significantly higher than the typical values used for kinetic tests in TGA (i.e., around 2−3 mg), was chosen to compensate for the sintering effect produced by this type of device upon the external surface of the raw meals over multiple calcination/carbonation cycles.[44] In these tests, the sample was heated up to 650 °C in the presence of 10 vol % CO_2 in air (gas velocity of 0.09 m/s). Under these conditions, the buoyant force was determined taking care not to calcine the sample. Once both the temperature and weight were stable, the atmosphere was switched to 100 vol % air after which the sample was heated up to 900 °C. This temperature was then maintained for periods of between 1 and 10 min (depending on the test), during which the carbonate present in the solids was calcined. It should be noted that calcination was performed while the sample was heated, as the heating step was carried out without the presence of CO_2 in the atmosphere. This resulted in a higher conversion of calcium to silicates.[39] The sample was then cooled down to 650 °C in air. Once the temperature and weight of the sample were stabilized, carbonation was performed with a gas containing 10 vol % CO_2 in air. The carbonation time was extended for 10 min in order to ensure the maximum possible CO_2 carrying capacity in each cycle (X_N).

To quantify the amount of belite formed from the calcium carbonate (X_{Bb}) nonisothermal tests were carried out with initial solids samples of around 2 mg and 100 vol % CO_2 in order to avoid the calcination of the $CaCO_3$. In these tests the temperature was increased at heating rates of between 5 °C/min and 30 °C/min until a final temperature ranging between 800 and 900 °C was reached. The maximum temperature was maintained for 10 min. The weight loss (after 700 °C) was assumed to be caused solely by $CaCO_3$ reacting with SiO_2 to form Ca_2SiO_4. As a result, the conversion of $CaCO_3$ to belite

DOI: 10.1021/acs.iecr.9b00813
Ind. Eng. Chem. Res. 2019, 58, 5445−5454

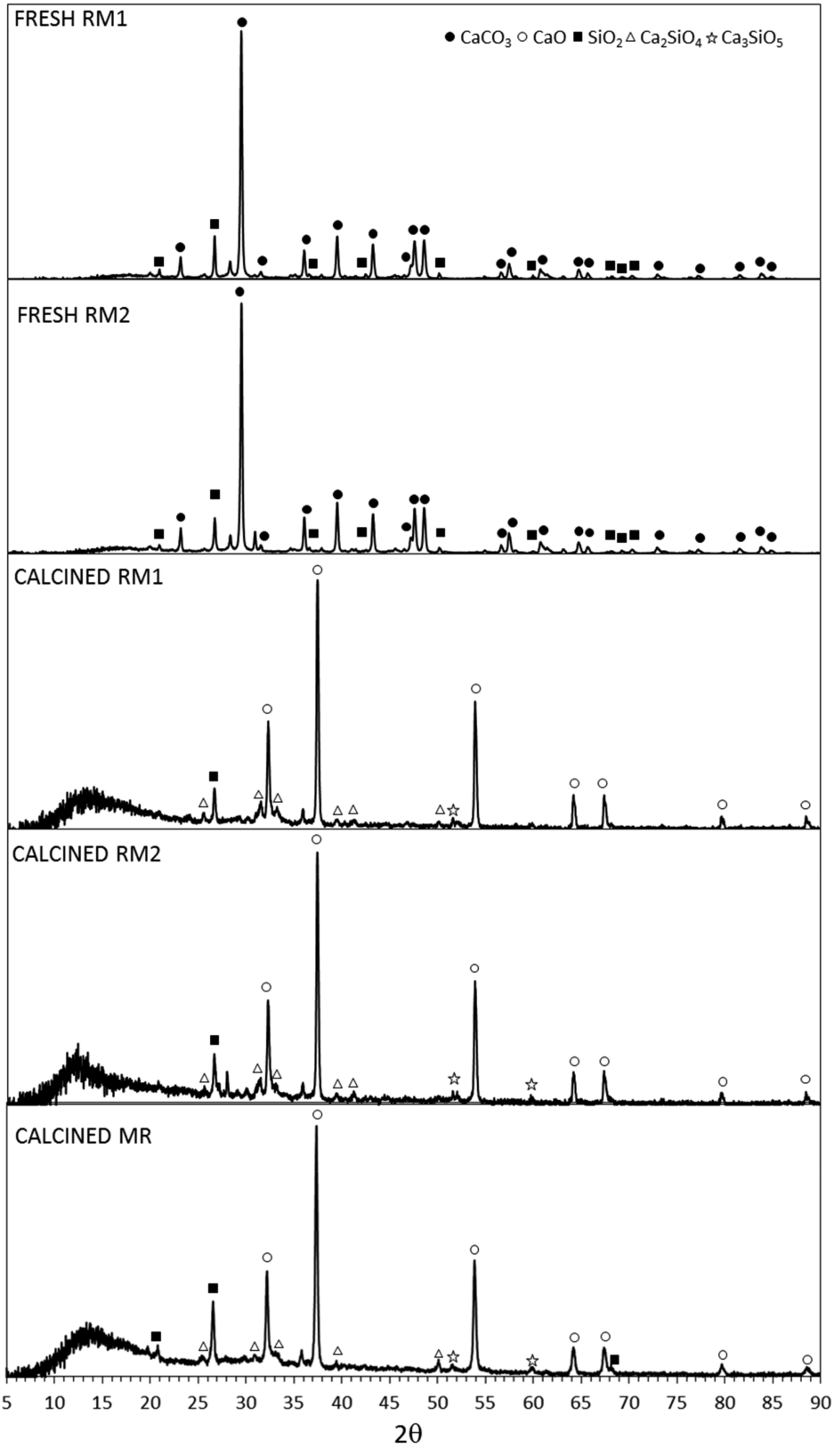

Figure 2. XRD spectra of the Ca−Si materials before and after calcination at 900 °C in air for 10 min.

(X_{Bb}) could be measured directly from the weight loss of the samples.

During the formation of belite from CaO (eq 2) the weight of the solid remains stable. Consequently, the conversion of CaO to Ca_2SiO_4 (X_{Ba}) cannot be estimated directly from TGA measurements. In this case, the conversion is therefore calculated by assuming that the decrease in the CO_2 carrying capacity of the samples is caused exclusively by the formation

DOI: 10.1021/acs.iecr.9b00813
Ind. Eng. Chem. Res. 2019, 58, 5445−5454

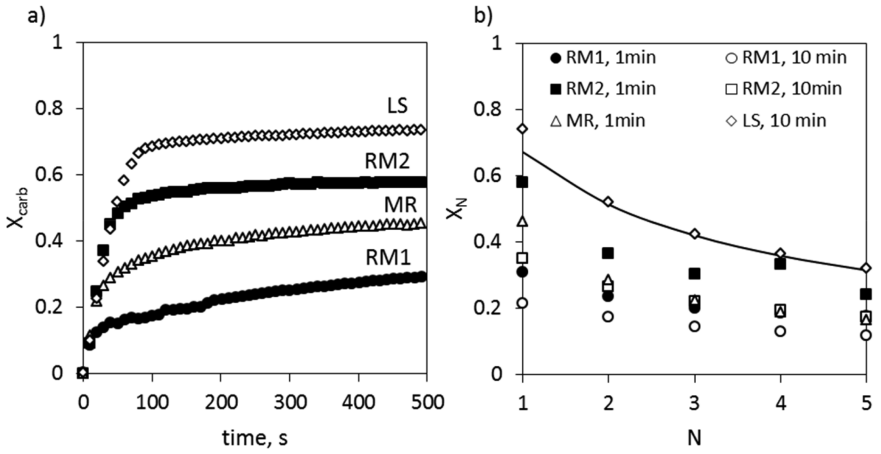

Figure 3. (a) Evolution of the CO_2 carrying capacity after the first calcination carried out at 900 °C during 1 min in air (carbonation at 650 °C with 10 vol % CO_2 in air). (b) Effect of calcination time on the maximum CO_2 carrying capacity through consecutive carbonation and calcination cycles (black line: eq 4 where k = 0.57 and X_r = 0.06).

of belite. The total amount of CaO converted to belite (X_B) can then be calculated from eq 3.

$$X_B = 1 - \frac{X_{carb}}{X_{max}} \quad (3)$$

where X_{carb} is the carbonation conversion measured at the end of the carbonation period and X_{max} is the degree of carbonation that should be achieved if no belite is formed. During the heating period before the onset of the calcination temperatures, a small fraction of belite may be formed from $CaCO_3$ (X_{Bb}), according to eq 1, which can be estimated using the model described in the next section. The belite formed from CaO (X_{Ba}) can then be calculated from the difference between the total conversion to belite (X_B) and X_{Bb}. In these tests, samples of around 2 mg were first heated up to 650 °C, while a gas stream (gas velocity of 0.09 m/s) containing 10 vol % CO_2 in air was fed into the TGA. This operation allowed the buoyancy at this temperature to be determined. Next, each sample was heated in the presence of 100 vol % CO_2 until the calcination temperature was reached. The gaseous feed was then switched to 100 vol % air (to initiate the calcination stage) and the temperature was maintained for a period of time ranging from 0.5 to 200 min. Calcination temperatures between 840 and 920 °C were applied. Afterward, the samples were cooled down to 650 °C in an air atmosphere and then carbonated at this temperature by feeding in a gas mixture consisting of 10 vol % CO_2 in air for 5 min. The carbonation conversion (X_{carb}) was calculated at the end of this period. To determine carbonation conversion when no belite is formed (X_{max}), some tests were carried out following the procedure described above but performing the calcination stage at 800 °C for 1 min in order to minimize the formation of belite.

RESULTS AND DISCUSSION

The CO_2 carrying capacities of the raw meals RM1 and RM2 and those of the individual components of RM2 (i.e., LS and MR) were evaluated following the experimental procedure explained in the previous section (Figure 3). The CO_2 carrying capacity is defined as the molar conversion of CaO to $CaCO_3$ in relation to the total amount of moles of CaO initially present (X_{carb} = mol $CaCO_3$/mol CaO). The maximum carrying capacity (X_N) is assumed to be the molar conversion achieved at the end of the carbonation period. Figure 3a shows the evolution of the carbonation conversion of these materials after heating in the presence of air up to 900 °C, with this temperature being maintained for 1 min. As can be seen, all the curves obtained for the materials follow the typical trend for the carbonation of CaO from limestone.[35] After a period of rapid carbonation (kinetic stage), a relatively stable value was reached (diffusional control stage). The maximum carbonation conversion was measured after 10 min in each cycle because the tests were carried out under external diffusional resistance.

A maximum value of around 0.7 was obtained for LS in the first cycle. In the case of the marl MR, the transition between the kinetic and the diffusional stage was more gradual and a final conversion of about 0.46 was achieved. The carbonation conversion for RM2 (i.e., the mixture of LS and MR) showed an intermediate value of 0.58. Finally, the raw meal RM1 exhibited the lowest carbonation conversion (about 0.30). These results demonstrate that the presence of SiO_2 significantly reduces the CO_2 carrying capacity of the calcium-based materials after the first calcination/carbonation cycle. This is because part of the calcium present in the samples reacts with SiO_2 to form belite (see Figure 2) even if it is only for a very short time at high temperatures. Moreover, a higher level of aggregation of Ca and Si compounds seems to have a significant impact on the reactivity of the sorbents with CO_2, in agreement with previous results reported by Alonso et al.[38]

The fall in the maximum CO_2 sorption carrying capacity of the solids through consecutive carbonation and calcination cycles (X_N) is represented in Figure 3b. In the calcium looping system of a cement plant, the particles of raw meal will be subjected to a very low number of cycles due to the typically large makeup flows and purges required in the calciner.[31,32] For this reason, a maximum of only five cycles has been considered in this study. Although LS showed a reasonably high X_N value in the first cycle (i.e., 0.73), a typical deactivation was observed as the number of calcination/carbonation cycles increased (X_N of 0.32 in the fifth cycle). Very similar values of X_N for LS were obtained for calcination periods of 1 and 10 min (only the X_N values achieved after 10 min of calcination have been represented in Figure 3b for the sake of simplicity). The trend followed by the curve as the number of cycles increased can be expressed by the equation obtained by Grasa and Abanades[45] for natural limestones:

DOI: 10.1021/acs.iecr.9b00813
Ind. Eng. Chem. Res. 2019, 58, 5445−5454

$$X_N = \frac{1}{\left(\frac{1}{(1-X_r)} + kN\right)} + X_r \quad (4)$$

where k is the decay constant and X_r is the residual conversion. Both parameters take average values of 0.52 and 0.075 for a wide range of natural Ca-derived sorbents. In the particular case of LS, values of k = 0.57 and X_r = 0.06 were obtained (represented by the black line in Figure 3b).

In contrast, longer calcination periods have a great effect on the CO_2 sorption capacity of Ca−Si materials. A X_N value approximately 30% lower was obtained for RM2 when the time at high temperature was increased from 1 to 10 min. For periods of 1 min at 900 °C, the decay curve for RM2 could be fitted to eq 4 using the average parameters of limestones by assuming that a CaO molar fraction of 0.75 was available to react with CO_2. However, when the period at high temperature was extended to 10 min, a larger amount of CaO reacted with SiO_2 to form belite, leaving only a CaO molar fraction of 0.5 available in RM2 for the capture of CO_2. In the case of MR, the CaO molar conversion decreased more rapidly and the CO_2 carrying capacity decay curve after 1 min at 900 °C could be described by eq 4 using values of k = 1.45 and X_r = 0.044 (i.e., 2.5 times higher and 27% lower, respectively, compared to the fitting parameters calculated for LS). This means that only a CaO molar fraction of 0.49 was available for reacting with CO_2, assuming that this fraction behaved like the CaO from a typical natural limestone. Finally, RM1 suffered further deactivation during multicycling. Only 44% of the moles of CaO were available for carbonation after 1 min at 900 °C. This percentage decreased to 32% when RM1 was calcined for 10 min. These results show that it is the fraction of free CaO that determines in general the performance of the Ca-based material as CO_2 sorbent, as its behavior is similar regardless of the origin of the material (i.e., whether it comes from a limestone or from another CaO-based solid). Hence, the differences observed in the performance of the raw meals are mainly the result of the conversion of CaO and/or $CaCO_3$ to belite.

The amount of $CaCO_3$ converted to belite needs to be determined not only to quantify the loss of free calcium necessary for the CO_2 capture before calcination but also to be able to evaluate the results obtained by the TGA during the heating period until the calcination temperature is reached (between 3 and 15 min depending on the heating rate and the final temperature). The time scales used in these experiments are in principle longer than the residence times of most of the solids in the calciner of a cement plant (that have typical residence times of less than 1 min). However, by means of extended analyze over long periods it is possible to determine the formation of belite in particles of raw meal that can be subjected to high temperatures for several minutes in dead zones of the calciner or in other parts of the cement plant (hoppers, feeding systems, etc).

As explained in the Experimental Section, during these TGA tests the samples are heated from room temperature up to a temperature range 800−900 °C. Figure 4 shows the evolution of sample weights with RM1 and synthetic calcium carbonate (100 wt % $CaCO_3$) in the presence of 100 vol % CO_2 at a heating rate of 5 °C/min (T_{max} = 900 °C). It can be seen that the weight of $CaCO_3$ remained stable throughout the test, indicating the absence of calcination. However, the sample of RM1 lost weight at temperatures above 500 °C, where clay

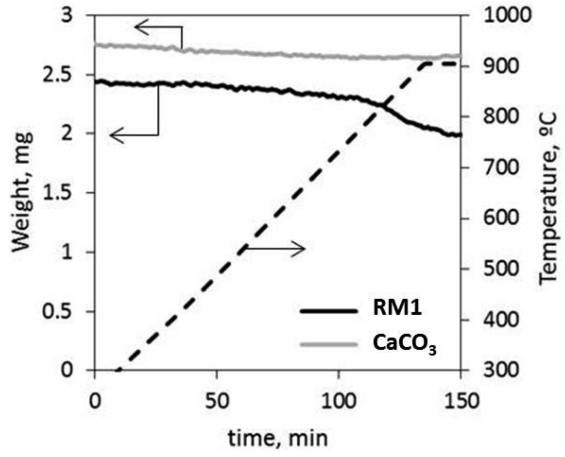

Figure 4. Evolution with time and temperature of sample weights of RM1 and synthetic $CaCO_3$ during TGA tests carried out with 100 vol % CO_2.

minerals contained in the RM1 suffered dehydroxylation reactions.[42] There was then an increase in the weight loss at temperatures of around 740 °C, which means that part of the calcium carbonate present in the raw meal reacted with SiO_2 to form belite in accordance with eq 1.

Figure 5 shows the results of tests carried out under atmospheres of pure CO_2 at a heating rate of 30 °C/min using different final temperatures. The figure shows that the $CaCO_3$ conversion to belite was favored at higher temperatures, especially in the case of RM1. At 900 °C, a value for X_{Bb} of about 0.26 was obtained in RM1 after 15 min (compared to a conversion of about 0.22 in RM2 under the same conditions). As the temperature decreased, the formation of belite from $CaCO_3$ was similar in both raw meals. In fact, exactly the same conversion was achieved in both samples at 800 °C (i.e., 0.09). However, the formation of belite began at lower temperatures in RM1. Belite was already detected in RM1 at temperatures around 730 °C, whereas this calcium silicate did not appear in RM2 until a temperature of about 770 °C was reached.

As can be seen in Figure 5, the CaO molar conversions to Ca_2SiO_4 lie within a narrow range. For this reason, the traditional methods for estimating the kinetic parameters from TGA experiments are not applicable.[46] Instead, a graphical method as described by these authors was used to identify the type of model required when only isothermal data are available. On the basis of this method, the 3D-diffusion model originally proposed by Jander and Hoffmann[47] was chosen to obtain the best fitting of all the experimental data (eq 5). The model was fitted to each raw meal, and the calculated parameters are shown in Table 2.

$$X_{Bb} = 1 - [1 - (k_{Bb}t)^{1/2}]^3 \quad (5)$$

where k_{Bb} is the reaction rate coefficient for belite formation from $CaCO_3$, which is assumed to have an Arrhenius dependence with temperature. Values of 7.09×10^3 s^{-1} and 195 kJ/mol were determined from the nonisothermal tests carried out with RM1 (4.58×10^3 s^{-1} and 194 kJ/mol for RM2). As can be seen in Figure 5a, the model describes accurately the extent of belite formation from $CaCO_3$ in RM1 at temperatures between 800 and 900 °C for solid conversions of up to 0.25. However, only very low conversions to belite (below 0.06) were predicted accurately in the case of RM2 (see Figure 5b). For higher solids conversions, the theoretical

DOI: 10.1021/acs.iecr.9b00813
Ind. Eng. Chem. Res. 2019, 58, 5445−5454

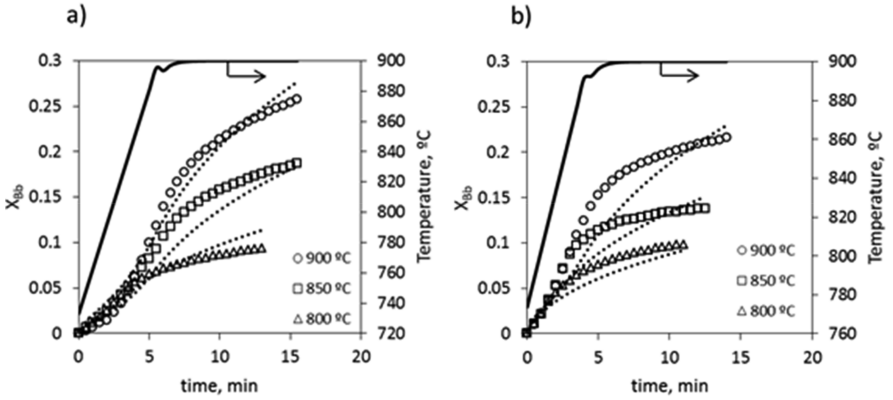

Figure 5. Conversion of $CaCO_3$ to belite before calcination and the temperature profile (at a heating rate of 30 °C/min): (a) RM1, (b) RM2. The dotted lines represent the model predictions.

Table 2. Kinetic Parameters for the Reactions of Belite Formation from CaO and $CaCO_3$

material	K_{0Ba} (s^{-1})	E_a (kJ/mol)
RM1	6.61×10^{10}	325
RM2	4.35×10^{10}	325
MR	5.13×10^{10}	325
material	K_{0Bb} (s^{-1})	E_a (kJ/mol)
RM1	7.09×10^{3}	195
RM2	4.58×10^{3}	194

calculations were significantly lower than the X_{Bb} measured experimentally. This is probably due to the different levels of Ca−Si aggregation in RM2 (mixture of a limestone and a marl).

On the other hand, the most relevant reaction regarding the formation of belite in raw meals is that produced from CaO after a calcination period (eq 2). As pointed out in the Experimental Section, this reaction path was studied by means of isothermal experiments at temperatures between 815 and 920 °C, assuming that the decay in the CO_2 sorption capacity was produced exclusively as a result of the formation of belite (the production of other calcium silicates at these temperatures is negligible). The effect of the calcination temperature on the conversion of CaO to Ca_2SiO_4 (X_{Ba}) is represented in Figure 6.

The experimental results indicate that higher temperatures during the calcination favor the formation of belite in both RM1 and RM2. In general, higher X_{ba} values were obtained in RM1, indicating that a greater aggregation of Ca and Si atoms in the raw meals seems to favor the formation of belite. When the calcination was carried out at 840 °C, a maximum solids conversion (X_{Ba}) of 0.23 was achieved in RM2 after 20 min. Only 2 min were needed in RM1 to achieve a similar degree of belite formation at the same calcination temperature. On the other hand, when the calcination temperature increased up to 920 °C, a solid conversion to belite of about 0.5 was observed in RM2 after 10 min, whereas the same X_{Ba} was reached in RM1 at a lower calcination temperature (890 °C) in barely 4 min.

These experimental data were fitted to the model proposed by Jander and Hoffmann[47] in order to estimate the kinetic parameters needed for the reaction to form belite from CaO (eq 6).

$$X_{Ba} = 1 - [1 - (k_{Ba}t)^{1/2}]^3 \quad (6)$$

where the parameter k_{Ba} is the reaction rate coefficient which follows an Arrhenius dependence on temperature. In a first fitting exercise for RM1, a value of 328 kJ/mol was obtained for the activation energy, which is very close to that reported by Weisweiler and Osen[41] (i.e., 325 kJ/mol) for the same

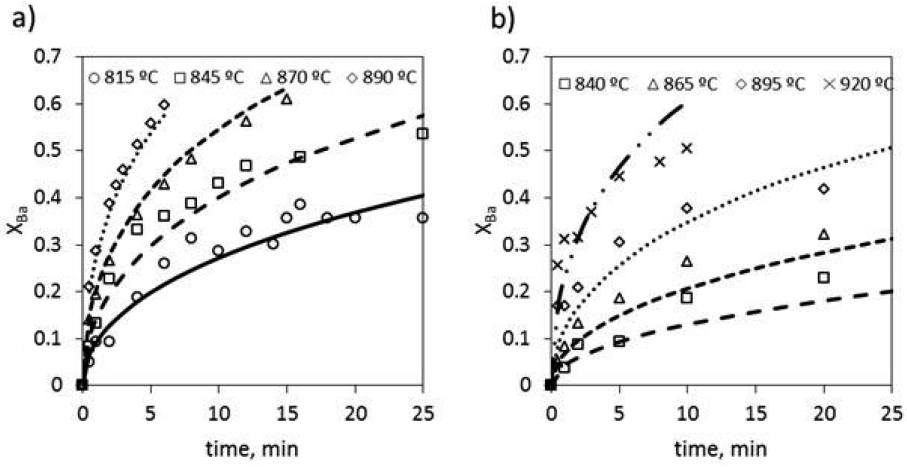

Figure 6. Effect of the calcination temperature on the conversion of CaO to belite (after calcination) at temperatures between 815 and 920 °C: (a) RM1, (b) RM2. Lines correspond to the model predictions.

DOI: 10.1021/acs.iecr.9b00813
Ind. Eng. Chem. Res. 2019, 58, 5445−5454

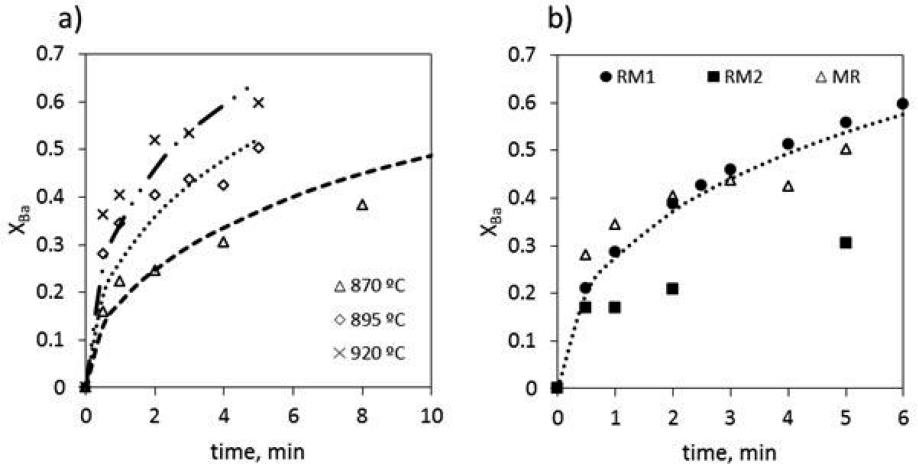

Figure 7. (a) Effect of the calcination temperature on the conversion of CaO to belite in MR (lines correspond to the model predictions). (b) Evolution of belite formation at 895 °C in the Ca−Si solids tested in this work (the line corresponds to the theoretical predictions made by the model assuming the kinetic parameters calculated for RM1).

reaction at the temperature range between 1000 and 1400 °C. Hence, this activation energy value was considered valid for the temperatures studied in the present work, and therefore, the only fitting parameter of the kinetic model was the pre-exponential factor characteristic of each material. The results are listed in Table 2.

As can be seen from Figure 6a, the model represents with reasonable precision the evolution of the solids conversion (X_{Ba}) in RM1 at every temperature tested, even for reaction times of up to 20 min and for X_{Ba} of up to 0.6. However, Figure 6b reveals that the resulting model tends to underestimate the solids conversion at temperatures below 900 °C for RM2. Again this may be due to the different nature of RM1 (marl) and RM2 (mixture of marl and limestone), as explained above.

In the case of MR (the marl component of the raw meal RM2) in Figure 7a, a reasonably good description of the evolution of belite formation from CaO at temperatures between 870 and 920 °C was obtained using the model, assuming an activation energy of 325 kJ/mol and the pre-exponential factor k_0 as the only fitting parameter for the kinetic equation. A value of 5.13×10^{10} s^{-1} was obtained, which lies between the values calculated for RM1 and RM2, as can be seen in Table 2.

In Figure 7b, the evolution of solids conversion to belite at 895 °C is represented for the Ca−Si materials tested in the present work. As can be seen, both RM1 and MR followed a very similar trend during the first minutes of the experiments. Short residence times of a few minutes are expected for the raw meal particles inside the calciner of a large-scale cement plant. The model including the kinetic parameters calculated for RM1 predicted reasonably well not only the degree of belite conversion in RM1 but also that in MR. However, the belite formation rate in RM2 was significantly lower than the values obtained for the other materials with higher level of Ca−Si aggregation. A more complex kinetic model would be needed to quantify more accurately the formation of calcium silicate in the conditions of calcium looping using raw meals derived from mixtures of solids of a different nature.

CONCLUSIONS

Compared to natural limestones, calcined raw meals show a more complex behavior as CO_2 sorbent due to the formation of belite (Ca_2SiO_4) which reduces the amount of CaO available for reacting with CO_2. Carbonation tests revealed significant reductions in the CO_2 sorption capacity of raw meals of different nature after the first calcination/carbonation cycle. Belite formed rapidly, even for calcination periods of only 1 min, especially in raw meals with higher level of aggregation of Ca and Si compounds. Tests carried out in thermogravimetric analyzers show that a certain amount of $CaCO_3$ can be directly converted to Ca_2SiO_4 at temperatures below 900 °C. However, the most important reaction for the formation of belite in raw meals is that between CaO and SiO_2 (i.e., after calcination). The 3D-diffusion model proposed by Jander and Hoffmann was able to predict with precision the conversion of $CaCO_3$ to belite in a marl-type raw meal (RM1) at temperatures between 800 and 900 °C and solid conversions of up to 0.20. On the other hand, this model was only able to represent very low levels of belite conversion (below 0.05) in raw meal obtained by mixing marl and limestone (RM2). This model was also applied to describe the formation of belite from CaO. The activation energy for this reaction in this temperature range is consistent with data reported in the literature on belite formation in CaO/SiO_2 materials at higher temperatures. Therefore, it can be inferred that the differences in the reaction rates between materials rely on the pre-exponential factors, directly related to the degree of Ca and Si aggregation in the materials. The kinetic model was found to represent reasonably well the evolution of solids conversion to belite in RM1 and MR at every temperature tested, even for reaction times of up to 20 min and for X_{Ba} values up to 0.6. However, this does not apply to the mixed material (RM2), where the conversion of CaO to belite was significantly lower due to the different levels of aggregation of Ca and Si in the raw meal.

AUTHOR INFORMATION

Corresponding Author

*Tel: +34 985 11 90 90. E-mail: jramon@incar.csic.es.

ORCID

Mónica Alonso: 0000-0002-1955-9432

DOI: 10.1021/acs.iecr.9b00813
Ind. Eng. Chem. Res. 2019, 58, 5445−5454

José Ramón Fernández: 0000-0001-9801-7043

Notes

The authors declare no competing financial interest.

■ ACKNOWLEDGMENTS

This study has been funded by the European Union's Horizon 2020 Research and Innovation Programme under Grant Agreement 764816 (CLEANKER Project) and by the Spanish Ministry of Economy, Industry and Competitivity (Grant ENE2015-68885-C2-1-R). We also acknowledge support of the publication fee by the CSIC Open Access Publication Support Initiative through its Unit of Information Resources for Research (URICI).

■ NOTATION

dp_S = Sauter diameter (μm)
dp_V = mean volumetric diameter (μm)
dp_{50} = median diameter (μm)
E_a = activation energy (kJ/mol)
k = decay constant (s^{-1})
k_{Ba} = reaction rate coefficient for belite formation from CaO (s^{-1})
k_{Bb} = reaction rate coefficient for belite formation from $CaCO_3$ (s^{-1})
k_0 = pre-exponential factor of the Arrhenius equation (s^{-1})
N = number of carbonation/calcination cycles
t = time (s)
X_B = total conversion of CaO to belite (mol belite/mol Ca)
X_{Ba} = molar conversion of CaO to belite (mol belite/mol Ca)
X_{Bb} = molar conversion of $CaCO_3$ to belite (mol belite/mol Ca)
X_{carb} = carbonation conversion at the end of the carbonation step (mol CO_2/mol Ca)
X_{max} = maximum carbonation conversion if no belite formed (mol CO_2/mol Ca)
X_N = carbonation conversion in cycle N (mol CO_2/mol Ca)
X_r = residual conversion (mol CO_2/mol Ca)

■ REFERENCES

(1) Andrew, R. M. Global CO_2 emissions from cement production. *Earth System Science Data* **2018**, *10*, 195−217.
(2) *IEA Technology Roadmap, Low-Carbon Transition in the Cement Industry*; International Energy Agency, 2018.
(3) Hills, T.; Leeson, D.; Florin, N.; Fennell, P. Carbon capture in the cement industry. Technologies, progress and retrofitting. *Environ. Sci. Technol.* **2016**, *50*, 368−377.
(4) Bosoaga, A.; Masek, O.; Oakey, J. E. CO_2 Capture Technologies for Cement Industry. *Energy Procedia* **2009**, *1*, 133−140.
(5) Vatopoulos, K.; Tzimas, E. Assessment of CO_2 capture technologies in cement manufacturing process. *J. Cleaner Prod.* **2012**, *32*, 251−261.
(6) *ECRA CCS Project. Report on Phase III*; European Cement Research Academy, 2012.
(7) Rodriguez, N.; Alonso, M.; Grasa, G.; Abanades, J. C. Process for capturing CO_2 arising from the calcination of the $CaCO_3$ used in cement manufacture. *Environ. Sci. Technol.* **2008**, *42*, 6980−6984.
(8) Valverde, J. M. Ca-based synthetic materials with enhanced CO_2 capture efficiency. *J. Mater. Chem. A* **2013**, *1*, 447−468.
(9) Boot-Handford, M. E.; Abanades, J. C.; Anthony, E. J.; Blunt, M. J.; Brandani, S.; Mac Dowell, N.; Fernández, J. R.; Ferrari, M. C.; Gross, R.; Hallett, J. P.; Haszeldine, R. S.; Heptonstall, P.; Lyngfelt, A.; Makuch, Z.; Mangano, E.; Porter, R. T. J.; Pourkashanian, M.; Rochelle, G. T.; Shah, N.; Yao, J. G.; Fennell, P. S. Carbon capture and storage update. *Energy Environ. Sci.* **2014**, *7*, 130−189.
(10) Erans, M.; Manovic, V.; Anthony, E. J. Calcium looping sorbents for CO_2 capture. *Appl. Energy* **2016**, *180*, 722−742.
(11) Martínez, I.; Grasa, G.; Parkkinen, J.; Tynjälä, T.; Hyppänen, T.; Murillo, R.; Romano, M. C. Review and research needs of Ca-Looping systems modelling for post-combustion CO_2 capture applications. *Int. J. Greenhouse Gas Control* **2016**, *50*, 271−304.
(12) Arias, B.; Diego, M. E.; Abanades, J. C.; Lorenzo, M.; Diaz, L.; Martínez, D.; Alvarez, J.; Sánchez-Biezma, A. Demonstration of steady state CO_2 capture in a 1.7MWth calcium looping pilot. *Int. J. Greenhouse Gas Control* **2013**, *18*, 237−245.
(13) Chang, M. H.; Huang, C. M.; Liu, W. H.; Chen, W. C.; Cheng, J. Y.; Chen, W.; Wen, T. W.; Ouyang, S.; Shen, C. H.; Hsu, H. W. Design and Experimental Investigation of Calcium Looping Process for 3-kWth and 1.9-MWth Facilities. *Chem. Eng. Technol.* **2013**, *36*, 1525−1532.
(14) Ströhle, J.; Junk, M.; Kremer, J.; Galloy, A.; Epple, B. Carbonate looping experiments in a 1 MWth pilot plant and model validation. *Fuel* **2014**, *127*, 13−22.
(15) Arias, B.; Diego, M. E.; Méndez, A.; Alonso, M.; Abanades, J. C. Calcium looping performance under extreme oxy-fuel combustion conditions in the calciner. *Fuel* **2018**, *222*, 711−717.
(16) Abanades, J. C.; Arias, B.; Lyngfelt, A.; Mattisson, T.; Wiley, D. E.; Li, H.; Ho, M. T.; Mangano, E.; Brandani, S. Emerging CO_2 capture systems. *Int. J. Greenhouse Gas Control* **2015**, *40*, 126−166.
(17) Dean, C. C.; Dugwell, D.; Fennell, P. S. Investigation into potential synergy between power generation, cement manufacture and CO_2 abatement using the calcium looping cycle. *Energy Environ. Sci.* **2011**, *4*, 2050−2053.
(18) Romano, M. C.; Spinelli, M.; Campanari, S.; Consonni, S.; Cinti, G.; Marchi, M.; Borgarello, E. The calcium looping process for low CO_2 emission cement and power. *Energy Procedia* **2013**, *37*, 7091−7099.
(19) Telesca, A.; Calabrese, D.; Marroccoli, M.; Tomasulo, M.; Valenti, G. L.; Duelli, G.; Montagnaro, F. Spent limestone sorbent from calcium looping cycle as a raw material for the cement industry. *Fuel* **2014**, *118*, 202−205.
(20) Rodriguez, N.; Murillo, R.; Alonso, M.; Martinez, I.; Grasa, G.; Abanades, J. C. Analysis of a Process for Capturing the CO_2 Resulting from the Precalcination of Limestone in a Cement Plant. *Ind. Eng. Chem. Res.* **2011**, *50*, 2126−2132.
(21) Romeo, L. M.; Catalina, D.; Lisbona, P.; Lara, Y.; Martinez, A. Reduction of greenhouse gas emissions by integration of cement plants, power plants, and CO_2 capture systems. *Greenhouse Gases: Sci. Technol.* **2011**, *1*, 72−82.
(22) Rodriguez, N.; Murillo, R.; Abanades, J. C. CO_2 Capture from Cement Plants Using Oxyfired Precalcination and/or Calcium Looping. *Environ. Sci. Technol.* **2012**, *46*, 2460−2466.
(23) Ozcan, D. C.; Ahn, H.; Brandani, S. Process integration of a Ca-looping carbon capture process in a cement plant. *Int. J. Greenhouse Gas Control* **2013**, *19*, 530−540.
(24) Romano, M. C.; Spinelli, M.; Campanari, S.; Consonni, S.; Marchi, M.; Pimpinelli, N.; Cinti, G. The Calcium looping process for low CO_2 emission cement plants. *Energy Procedia* **2014**, *61*, 500−503.
(25) De Lena, E.; Spinelli, M.; Martínez, I.; Gatti, M.; Scaccabarozzi, R.; Cinti, G.; Romano, M. C. Process integration study of tail-end Ca-Looping process for CO_2 capture in cement plants. *Int. J. Greenhouse Gas Control* **2017**, *67*, 71−92.
(26) De Lena, E.; Spinelli, M.; Gatti, M.; Scaccabarozzi, R.; Campanari, S.; Consonni, S.; Cinti, G.; Romano, M. C. Techno-economic analysis of calcium looping processes for low CO_2 emission cement plants. *Int. J. Greenhouse Gas Control* **2019**, *82*, 244−260.
(27) Atsonios, K.; Grammelis, P.; Antiohos, S. K.; Nikolopoulos, N.; Kakaras, E. Integration of calcium looping technology in existing cement plant for CO_2 capture: Process modeling and technical considerations. *Fuel* **2015**, *153*, 210−223.

DOI: 10.1021/acs.iecr.9b00813
Ind. Eng. Chem. Res. 2019, 58, 5445−5454

(28) Fernández, J. R.; Abanades, J. C. CO_2 capture from the calcination of $CaCO_3$ using iron oxide as heat carrier. *J. Cleaner Prod.* **2016**, *112*, 1211−1217.
(29) Diego, M. E.; Arias, B.; Abanades, J. C. Analysis of a double calcium loop process configuration for CO_2 capture in cement plants. *J. Cleaner Prod.* **2016**, *117*, 110−121.
(30) Spinelli, M.; Martínez, I.; Romano, M. C. One-dimensional model of entrained-flow carbonator for CO_2 capture in cement kilns by Calcium looping process. *Chem. Eng. Sci.* **2018**, *191*, 100−114.
(31) Arias, B.; Alonso, M.; Abanades, C. CO_2 Capture by Calcium Looping at Relevant Conditions for Cement Plants: Experimental Testing in a 30 kWth Pilot Plant. *Ind. Eng. Chem. Res.* **2017**, *56*, 2634−2640.
(32) Hornberger, M.; Spörl, R.; Scheffknecht, G. Calcium looping for CO_2 capture in cement plants - pilot scale test. *Energy Procedia* **2017**, *114*, 6171−6174.
(33) Turrado, S.; Arias, B.; Fernández, J. R.; Abanades, J. C. Carbonation of Fine CaO Particles in a Drop Tube Reactor. *Ind. Eng. Chem. Res.* **2018**, *57*, 13372−13380.
(34) Blamey, J.; Anthony, E. J.; Wang, J.; Fennell, P. S. The calcium looping cycle for large-scale CO_2 capture. *Prog. Energy Combust. Sci.* **2010**, *36*, 260−279.
(35) Barker, R. The reversibility of the reaction $CaCO_3 \rightleftarrows CaO + CO_2$. *J. Appl. Chem. Biotechnol.* **1973**, *23*, 733−742.
(36) Alsop, P. A. *The Cement Plant Operations Handbook: For Dry-Process Plants*, 6th ed.; Tradeship Publications Limited, 2014.
(37) Pathi, S. K.; Lin, W.; Illerup, J. B.; Dam-Johansen, K.; Hjuler, K. CO_2 capture by cement raw meal. *Energy Fuels* **2013**, *27*, 5397−5406.
(38) Alonso, M.; Álvarez Criado, Y.; Fernández, J. R.; Abanades, C. CO_2 Carrying Capacities of Cement Raw Meals in Calcium Looping Systems. *Energy Fuels* **2017**, *31*, 13955−13962.
(39) Alonso, M.; Hornberger, M.; Spörl, R.; Scheffknecht, G.; Abanades, C. Characterization of a Marl-Type Cement Raw Meal as CO_2 Sorbent for Calcium Looping. *ACS Omega* **2018**, *3*, 15229−15234.
(40) Wolter, A. Phase composition of calcined raw meal. *8th International Congress on the Chemistry of Cement*, Río de Janeiro, Brazil; 1986; pp 89−94.
(41) Weisweiler, W.; Osen, E. J.; Höfer, H. Kinetic studies in the $CaO\text{-}SiO_2$- system part II reaction rate constants and activation energies of selected diffusion couples. *Cem. Concr. Res.* **1988**, *18*, 55−62.
(42) Taylor, H. F. W. *Cement Chemistry*; Thomas Telford: London, 1997.
(43) Criado, Y. A.; Alonso, M.; Abanades, J. C. Kinetics of the $CaO/Ca(OH)_2$ Hydration/Dehydration Reaction for Thermochemical Energy Storage Applications. *Ind. Eng. Chem. Res.* **2014**, *53*, 12594−12601.
(44) Alonso, M.; Criado, Y. A.; Abanades, J. C.; Grasa, G. Undesired effects in the determination of CO_2 carrying capacities of CaO during TG testing. *Fuel* **2014**, *127*, 52−61.
(45) Grasa, G. S.; Abanades, J. C. CO_2 capture capacity of CaO in long series of carbonation/calcination cycles. *Ind. Eng. Chem. Res.* **2006**, *45*, 8846−8851.
(46) Vyazovkin, S.; Burnham, A. K.; Criado, J. M.; Pérez-Maqueda, L. A.; Popescu, C.; Sbirrazzuoli, N. ICTAC Kinetics Committee recommendations for performing kinetic computations on thermal analysis data. *Thermochim. Acta* **2011**, *520*, 1−19.
(47) Jander, W.; Hoffmann, E. Reaktionen im festen Zustande bei höheren Temperaturen. XI. Mitteilung. Die Reaktion zwischen Calciumoxyd und Siliciumdioxyd. *Z. Anorg. Allg. Chem.* **1934**, *218*, 211−223.

DOI: 10.1021/acs.iecr.9b00813
Ind. Eng. Chem. Res. 2019, 58, 5445−5454